The Los Alamos Dynamic Radiation Environment Assimilation Model (DREAM) for Space Weather Specification and Forecasting

Geoffrey D. Reeves, Reiner H. W. Friedel, Yue Chen, Josef Koller, and Michael G. Henderson
Space Science and Applications Group
Mail Stop D-466
Los Alamos National Laboratory
Los Alamos, NM 87544

ABSTRACT

The Dynamic Radiation Environment Assimilation Model (DREAM) was developed at Los Alamos National Laboratory to assess, quantify, and predict the hazards from the natural space environment and the anthropogenic environment produced by high altitude nuclear explosions (HANE). DREAM was initially developed as a basic research activity to understand and predict the dynamics of the Earth's Van Allen radiation belts. It uses Kalman filter techniques to assimilate data from space environment instruments with a physics-based model of the radiation belts. DREAM can assimilate data from a variety of types of instruments and data with various levels of resolution and fidelity by assigning appropriate uncertainties to the observations. Data from any spacecraft orbit can be assimilated but DREAM was designed to function with as few as two spacecraft inputs: one from geosynchronous orbit and one from GPS orbit. With those inputs, DREAM can be used to predict the environment at any satellite in any orbit whether space environment data are available in those orbits or not. Even with very limited data input and relatively simple physics models, DREAM specifies the space environment in the radiation belts to a high level of accuracy. DREAM has been extensively tested and evaluated as we transition from research to operations. We report here on one set of test results in which we predict the environment in a highly-elliptical polar orbit. We also discuss long-duration reanalysis for spacecraft design, using DREAM for real-time operations, and prospects for 1-week forecasts of the radiation belt environment.

1. INTRODUCTION and DEFINITION OF COORDINTES

The Dynamic Radiation Environment Assimilation Model (DREAM) uses operationally-available observations and data assimilation techniques to specify the space environment globally in order to specify the hazards to space systems from the space environment. DREAM uses techniques and has applications that are, in many ways, similar to those in the more well-known Global Ionospheric Assimilation Models (GAIM). Data assimilation combines limited observations with physical models using techniques, such as Kalman filtering, that optimize the accuracy of the model output. Both models and observations are assumed to have uncertainties and generally the model output is neither completely consistent with the equations of the physical model or completely consistent with the data inputs but, rather, produces an output is optimized to minimize internal inconsistencies. As a hypothetical example, consider a physical model that only includes equations for straight line motion and apply it to observations of the orbit of a satellite around the Earth. Although the physical model is not perfectly accurate and the location of the satellite may be observed only intermittently, a data assimilation model will produce a trajectory that approximates the motion of the satellite. Importantly, better observations (e.g. more frequent or more precise) or of better models (e.g. circular arc segments) will not only improve the model output but the effect on reducing errors and optimizing the solution can be evaluated quantitatively. Furthermore, parameter estimation techniques applied to assimilative models can find and evaluate processes that are not explicit in the model – in the example of the satellite this could be orbital maneuvering.

The DREAM model applies these techniques to the problem of specifying the radiation environment in the Van Allen radiation belts. This radiation is in the form of electrons and protons that are trapped in the Earth's magnetic field and have energies that allow them to penetrate to the interior of satellites,

electronics, and sensors. The particles in the radiation belts produce adverse effects including total dose effects, charging/discharging, high backgrounds and false signals in detectors, single event effects, displacement damage, etc. The flux of protons and electrons and their distribution in energy (spectrum) determine the intensity of the radiation environment and effects on space systems can be produced by the current environment (e.g. bit flips), by the recent history of the environment (e.g. internal charging/discharging), or by the cumulative history of the environment experienced since launch (e.g. total dose).

A major challenge to modeling, to situational awareness, and to operations is that the fluxes in the radiation belt exhibit extreme variability. Fluxes can vary in magnitude by factors of 10^5 on time scales ranging from solar cycles (~11 years) to as little as a few minutes [1] but most variations happen on time scales ranging from hours to days. Fluxes also vary as a function of energy with different energies exhibiting quite different temporal variation and spatial distribution. Even though the radiation belts are so variable, assimilative modeling is helped by the fact that there are frequently strong correlations among fluxes measured at different locations. These correlations exist because the Earth's magnetic field guides the motion of charged particles (electrons and positive ions). Charged particles gyrate in circles around a particular magnetic field line. They also bounce back and forth along a magnetic field line between magnetic mirror points (Fig. 1). This means that the particles measured at any point on a field line can be specified by the distribution of particles at the magnetic equator – which is also the point where the field is furthest from the center of the Earth. We label that point by the parameter L which is measured in units of Earth radii (1 R_E = 6370 km). Particles at any point on the field line have the same L value which reduces the problem from a 3-dimensional volume to a 2-dimensional surface.

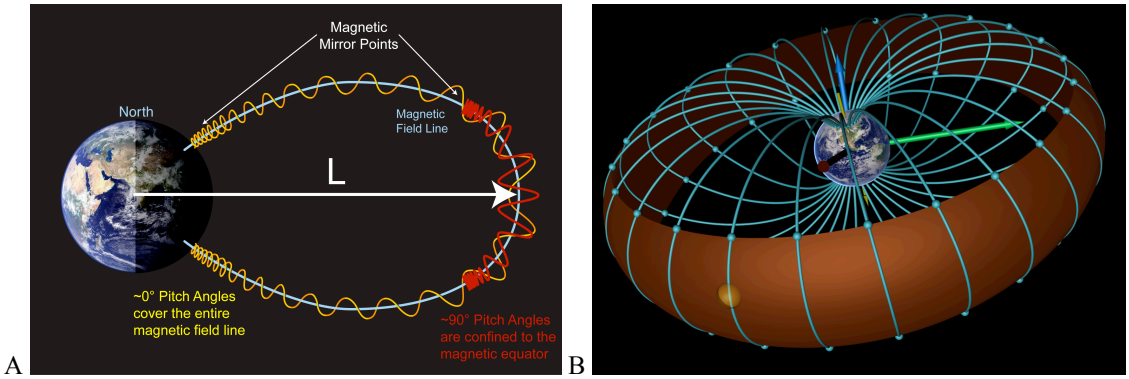

Fig 1. Motion of charged particles and the definition of "L". (A) Electrons and positive ions will gyrate around the magnetic field and will bounce along the field between magnetic mirror points which are determined by the local magnetic field strength and the particle's pitch angle. Therefore it is convenient to label any point on a magnetic field line with the same value of "L" which is defined as the radial distance to the magnetic equator and is measured in units of Earth radii (R_E). (B) Motion of charged particles on a "drift shell". This figure illustrates magnetic field lines and mirror points (blue) and the drift motion of charged particles around the Earth along a trajectory that traces a surface called a "drift shell". The magnetic field and drift shells change and are distorted by solar and geomagnetic activity.

Radiation belt dynamics are typically presented in the form of flux (at a particular energy) or dose as a function of time and L – which can be thought of as a "magnetic altitude". As a point of reference, geosynchronous orbit is at a geographic altitude of 35,000 km or 42,000 km geocentric radial distance, which corresponds to L ≈ 6.6. The GPS orbits have a radius of 26,000 km but are inclined so they cross the equator at L ≈ 4.2 but cross L values out to >10 as their orbit crosses field lines at higher and higher latitudes.

The Earth's magnetic field also causes charged particles to drift azimuthally around the Earth with electrons drifting East and ions drifting West. In a simple dipole magnetic field this drift motion would

describe a shell (a "drift-shell") with constant radius, L. The real geomagnetic field, though, is distorted by interaction with the solar wind and by internal electric currents that both vary with time. This distorts the drift shell (Fig. 1B) and makes it change with time and spacecraft location (latitude, longitude, radius). The distortion is most extreme during geomagnetic storms that are caused by enhanced solar activity. Geomagnetic activity is typically described in terms of two parameters: Dst, and Kp. Geomagnetic storms are indicated when Kp is high (e.g. Kp > 3) and when Dst is low (e.g. Dst < -50 nT: storms drive Dst more negative).

For this reason, the DREAM model includes a realistic, time-dependent, distorted magnetic field model that accurately represents the geomagnetic field and the motion of radiation belt particles in that field. Different models can be used depending on the required accuracy and the computational time required to calculate particle motion. We have implemented simple, computationally fast models such as the Tsyganenko 1989 (T89) model [2] as well as the more complex but more accurate Tsyganenko 2001 storm (T01S) model [3]. DREAM can also be run with a module that self-consistently calculates the distortion of the magnetic field due to ring current and plasma pressures during storms [4]. In all we have tested 9 geomagnetic field models and determined their ranges of validity and computational requirements to evaluate which models are appropriate for which applications. Results in this study use the T89 model.

The dynamic equations of motion for radiation belt particles in the Earths magnetic field (or magnetosphere) are specified based on the three particle motions described above (gyration, bounce, and drift) which are in turn represented by three magnetic invariant quantities designated μ, K, and L (or L* in more precise calculations) [5]. Physical modeling of the radiation belts first requires converting electron or ion flux at a particular spatial location and energy into a coordinate system defined by these magnetic invariants. The dynamic equations are solved for transport of particles, energization of the particles, losses out of the boundaries of the magnetosphere, and losses into the Earth's atmosphere. In the final step, we convert back from magnetic coordinates to flux, energy, and spatial coordinates to directly determine the environment at any point in the radiation belts and therefore the conditions at any particular satellite's location.

DREAM uses the radial diffusion equation to quantify particle transport. We use energy diffusion or phase space assimilation to represent processes that accelerate particles to higher energies. We allow particles to be lost out of the system by specifying the dynamic boundary of the magnetosphere (the magnetopause) as a function of geomagnetic and solar wind conditions. We apply different losses to the atmosphere in two different regions. Inside the high density plasmasphere ($L \approx 2$-4) we use a constant 10-day lifetime and outside the plasmasphere we use an activity-dependent lifetime parameterized by the Kp index. The plasmasphere and it's boundary are specified by a dynamic model that is also parameterized by Kp. The physical model and details of the assimilation can be found in [6-12].

2. HANE-PRODUCED RADIATION BELTS

The DREAM model also includes components that can model the production, trapping, and evolution of HANE-produced electrons [13]. Although that aspect is not discussed in detail in this paper we do note several important aspects of the DREAM-HANE model. In addition to new models of the HANE production of source electrons due to beta decay of radioactive debris, considerable care was used to calculate the magnetic trapping of those HANE-produced electrons. We model debris as it moves up or down the field line and determine, statistically, the location at which beta-decay electrons will be produced. Electrons produced at different points along the field will have different pitch angle distributions and will experience different fractions of trapping. DREAM is the first model to realistically evaluate trapping fractions as a function of burst location.

Once they are trapped in the geomagnetic field, HANE electrons are subject to all the same processes as the natural ambient electron population including transport, acceleration, and decay. Without actual HANE measurements to assimilate, DREAM assimilation uses measurements of the natural environment to determine which processes are operating at a given time and spatial location and then applies those processes to the evolution of HANE electrons. When ambient electrons are accelerated so are HANE electrons. Likewise the time-dependent decay of ambient electrons shows quantifies the decay rate of

HANE electrons. Different scenarios at different phases of the solar cycle or under different geomagnetic conditions can be numerically tested. We further note that if an actual HANE occurred it would be measured by the same sensors we use in this study and the assimilation methods of DREAM would fully specify the new enhanced radiation environment and could be used to predict the effects on specific satellite systems as we discuss below.

3. DREAM RESULTS

We describe here a test case that uses space environment instruments on GPS and geosynchronous satellites to calculate the global, three-dimensional, time-dependent radiation environment. We use an independent set of measurements from a different spacecraft in a completely different orbit to validate the model output.

The data that we assimilate in this example come from the LANL Synchronous Orbit particle Analyzers (SOPA) detectors on three geosynchronous satellites [14] and from the Burst Detector Dosimeter (BDD IIR) on GPS ns41[15]. (Although there are data available from at least one satellite in each of the GPS orbital planes, in this study we employ data from only one satellite in the constellation.) The data that we use to test and validate our global prediction comes from the Comprehensive Energetic Particle and Pitch Angle Distribution (CEPPAD) experiment on NASA's POLAR satellite [16].

It is important to emphasize that data from the POLAR satellite are not used in the assimilation in any way and are a completely independent validation set. Furthermore, POLAR is in a vastly different orbit from the input data sets. Geosynchronous orbit satellites are in a near 0 deg inclination circular orbit with radius of 6.6 R_E. GPS orbit is a circular 12-hr orbit with radius 4.2 RE and an inclination of 55 deg. POLAR is in an elliptical orbit with apogee at 9 R_E and perigee at ~1.5 R_E. During the interval studied here the orbit inclination was approximately 80 deg and apogee was at approximately -45 deg to the solar ecliptic plane.

Here we use the flux of 1 MeV electrons measured by POLAR as our test data set and we compare the predictions based on three radiation belt models: DREAM, CRRESELE, and AE8. The AE8 model [17] is the accepted international standard model. It represents an average compiled from statistical observations sorted by magnetic coordinates (L and B/B_0). AE8 is not a time-dependent model but there are slightly different versions for solar maximum or solar minimum. This study uses AE8min. The CRRESELE model [18] is based on observations taken in 1990-1991 by the joint USAF-NASA Combined Release and Radiation Effects Satellite (CRRES). It is a time-dependent model that is parameterized by geomagnetic activity (Kp) as well as magnetic coordinates.

Fig 2. shows the results of our calculations for the full year of 2005 when POLAR's orbit provided good observations of the region L>4. The top panel shows the 1 MeV electron fluxes measured by the POLAR satellite (in electrons/cm^2/s/sr/keV). The data are binned into 1-day increments with a spatial resolution of 0.5 R_E in L. The data appear sparse for a variety of reasons including our choice of magnetic parameters μ and K, removal of data when the detector was saturated, missing points in the data set, etc. The fluxes are observed to vary considerably both as a function of time and location. As expected, the peak of the electron belt is typically observed between L=4-5 with a steep drop-off in flux at higher L. Fluxes vary in response to geomagnetic activity (bottom panel) which exhibited a number of strong (Dst < -100 nT) and a few intense (Dst < -150 nT) storms in 2005.

The next three panels show the results from the three models: DREAM, AE8, and CRRESELE. All three models provide global specification of 1 MeV electron flux but model results are only plotted in bins where POLAR observations are available for direct comparison. As noted, the AE8 model shows no variation because it is an average, static model. The CRRES model, by design, scales with geomagnetic activity (Kp averaged over 15 days) and shows a reasonable correlation with POLAR observations. The DREAM model shows the most variation both in time and L and has the best correlation with the POLAR observations. While this is to be expected from a data assimilation model, the ability of DREAM to reproduce the fluxes at POLAR using very limited data from satellites in completely different orbits is rather remarkable.

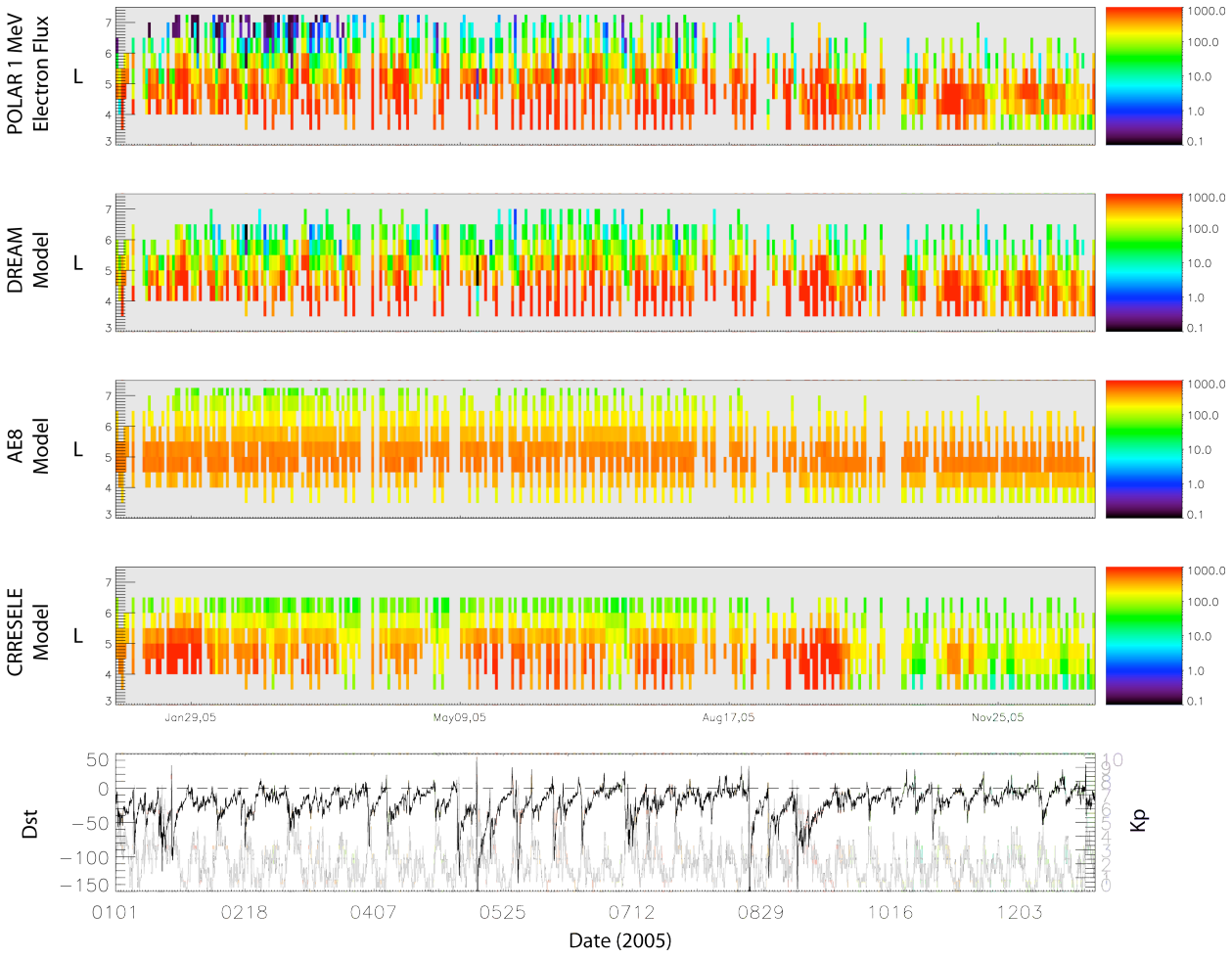

Fig 2. DREAM model results. The top 4 plots all show 1 MeV electron flux (color-coded with units of #/cm^2/s/sr/keV) as a function of time and L (radial distance from the center of the Earth in units of R_E = 6370 km). Data are binned in 1-day, 0.5 L intervals. From top to bottom the panels show flux measured by the POLAR satellite, flux predicted by the DREAM model, the AE8min model, and the CRRESELE model. The bottom panel shows geomagnetic activity measured by Kp (gray) and Dst (black). High levels of activity are indicated by large positive values of Kp and by large negative values of Dst. Data are for the year 2005.

In order to quantitatively compare model outputs we had to predict the space environment at a satellite that already had space environment sensors. Clearly this has little practical operational value. It should, however, be equally clear that the same techniques apply to predicting the space environment at satellites that do not have space environment sensors or even satellites with sensors that have limited energy coverage, poor energy or species resolution, poorly-known calibrations, or other limitations. Space situational awareness depends on knowing the environment at any satellite at any time – not just average or typical conditions and not just in those few orbits with operational space environment data.

Of course, once a data source such as POLAR (or any other satellite) has been used to test and validate the DREAM model it too becomes a source for assimilation. Using this “boot strap” approach our technology development plan aims to assimilate a broader array of space environment data to improve the accuracy and extend the boundaries of validity for the model: spatial limits and energy limits. We also continue to develop, apply, and test new physical models that will be particularly important for predictive space environmental awareness.

4. PREDICTION AND VALIDATION METRICS

The previous section presented a comparison between the observed 1 MeV fluxes at POLAR and the predictions for the same time period from DREAM, AE-8, and CRRESELE. Now we turn to metrics that can be used to validate our results and provide quantitative comparisons. In this section we evaluate the ability of the models to reproduce average conditions and their ability to predict variations. We also illustrate how data assimilation models can quantitatively evaluate the improvements gained by assimilating new data sources or by improving physical models.

First we look at the average fluxes. Fig 3. shows the electron flux as a function of L averaged over a full year – 2005, the same interval shown above. All three plots show, in black, the average profile of 1 MeV electron flux as a function of L measured by POLAR. The mean of the log(flux) is the solid curve and the standard deviation around the mean is shown with dotted curves. The average POLAR fluxes are compared to the average model fluxes as shown. Both the DREAM and CRRESELE averages are within a factor of 2 of the average POLAR fluxes and inside one standard deviation across the full range of L. Both show a profile that is very similar to the observations. The DREAM averages match best near L=4 and 6 and are worst at L<4 where no data were used in the model. CRRESELE and AE8 match best between L=4-5 where the peak fluxes are observed but the AE8 model systematically underestimates flux at lower L and overestimates flux at higher L (at least for this time period and this energy). The underestimate at low L is less than a factor of 2 but the overestimate at L=6 is a factor of 10 and continues to get worse at higher L.

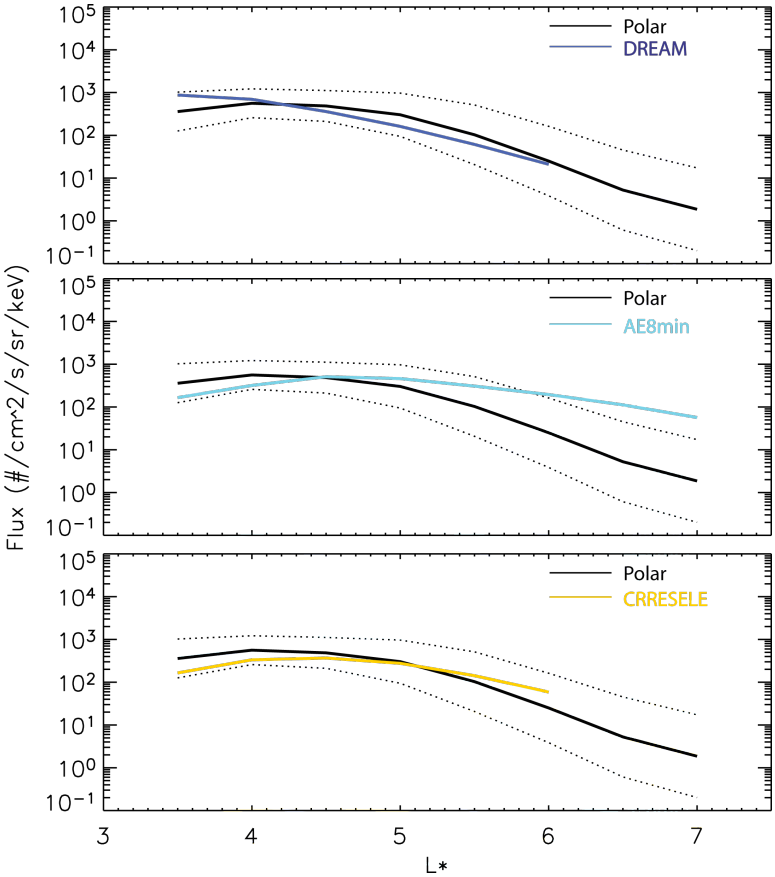

Fig. 3. Average flux values predicted by the models. Each panel shows the average and standard deviation of fluxes measured by POLAR as a function of L (geocentric radius). The average fluxes predicted by the DREAM, AE8, and CRRESELE models reproduce the average observations reasonably well with the exception of AE8 at high L values.

As one would hope, all three models are able to reproduce the average conditions with some degree of accuracy but where the DREAM data assimilation really shows its utility is in predicting the variation around the mean. A standard metric for measuring the ability to track variations is the prediction efficiency, PE, which is defined as

$$PE = 1 - \frac{\sum (m_i - o_i)^2}{\sum (o_i - \langle o \rangle)^2}$$

where m_i is the model output at time i, o_i is the observation at time i, and $< o >$ denotes the average value of the observations which is the average flux as shown in Fig 3. A perfect prediction is indicated when PE = 1 because, in that case, model matches the observations at every time i and $(m_i - o_i) = 0$. If the "model" simply assumes that the flux is equal to the average observed value then $m_i = < o >$ which gives a prediction efficiency of PE = 0. Positive values of PE indicate that the model predicts the variations better than assuming that flux is constant and negative values of PE mean that the model is worse.

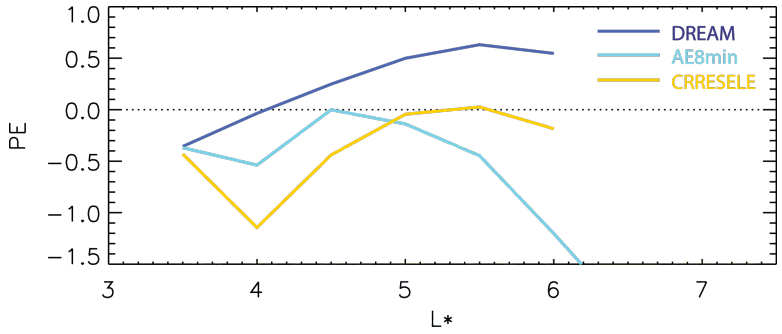

Fig. 4. Prediction efficiency. The prediction efficiency, PE (defined in the text), tests the ability of the model to predict the variation of fluxes around the mean. A prediction efficiency of 1 is perfect agreement at all times. Prediction efficiencies less than or equal to zero do not provide useful predictions of the time variation of the observations.

Fig. 4. shows the prediction efficiency for DREAM, AE8, and CRRESELE. Clearly the DREAM model excels at predicting the variation of electron flux observed by POLAR. For all values of L > 4, the prediction efficiency is positive and, as we noted above, this study did not include data at L < 4 because it only used data from GEO (L=6.6) and GPS (L>4.2) orbits. The CRRESELE model has a variable output that is scaled by geomagnetic activity but the fact that the prediction efficiency is negative at all L indicates that the variations are at the wrong times or are of the wrong magnitude. In this case it would be better to use the average value and not allow any time variation in the model. The AE8 model has no time variation so it may seem surprising that the prediction efficiency is not zero for all L. The reason it is negative for most values of L is that the AE8 value is not equal to the average observations. Where the AE8 and POLAR averages are equal (see Fig. 3) the prediction efficiency is zero. By applying a multiplicative factor to AE8 one could make the model match the observations at any given L but because the curves have different shapes they will only cross at one L and the prediction efficiency will still be less than or equal to zero for any satellite orbit.

Another highly desirable feature of data assimilation is that it has the ability to quantify the value of each component of the assimilative model: either the observations or the physical model used. Physicist typically assume that more data is better and that more sophisticated models will give more accurate results. For practical SSA applications though, it is best to use as little data and as computationally efficient a model as

required to still get an answer with sufficient accuracy and fidelity. The framework used by DREAM allows us to answer the questions "What do I gain by adding a new set of observations?", "Are the physical models sufficiently accurate?", or "What would I lose if one set of inputs becomes unavailable?" This ability enables cost-effective, informed decisions on R&D investment but, even more importantly, it gives us the ability to investigate which space weather architectures and which space environment sensors in which orbits provide the biggest bang for the buck.

Fig. 5. illustrates how we quantify where and how one set of observations affects the accuracy of space weather prediction using DREAM. The figure shows the DREAM assimilation for the last six months of 2002. The top panel shows the assimilation using the same geosynchronous and GPS observations as our 2005 validation interval. The locations where satellite observations were assimilated are shown with white dots. (In this case we only used values on the magnetic equator so GPS observations are at L≈4 and geosynchronous data are at L≈6.) The second panel shows the assimilation using only geosynchronous data with everything else the same. The bottom panel shows the ratio of the two model outputs as a function of L and time. The color bar is on a log scale with red (1) indicating that removing the GPS data produces a result that is 10 times too low and blue (-2) indicating that the result is 100 times too high.

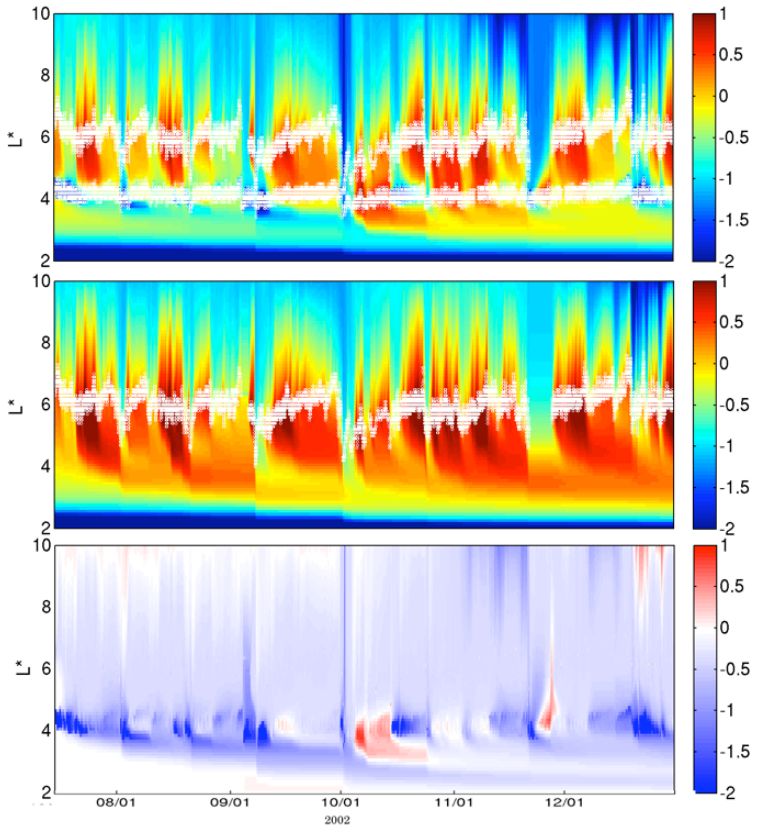

Fig. 5. DREAM assimilation results with and without GPS observations. Top: assimilation results (normalized equatorial Phase Space Density) using both geosynchronous and GPS measurements of radiation belt electron flux. Middle: the same but assimilating only geosynchronous data without GPS. Bottom: the log of the ratio of values determined with and without GPS data. Red values indicate where lack of GPS data causes a 10x underestimate and blue indicates a 100x overestimate.

An interesting feature of Kalman filter technique used by DREAM is that any assimilated data affects the global solution – not just the location of the satellite. Removing the GPS data from the assimilation affects the local region (L≈4) most strongly but errors are introduced throughout the system. In other words, it

would affect the predictions of the environment at any satellite orbit but it would affect predictions for MEO satellites the most severely.

5. PROSPECTS FOR 1-WEEK FORECASTS

We now turn our attention to uses of the DREAM model for real-time applications and for space weather forecasts. While retrospective analysis or "near real-time" specifications have many uses for assessing satellite anomalies, state-of-health, or survivability analysis, SSA applications also need to answer the question "What is happening at my satellite right now?" or the even more challenging question "What is likely to happen to my satellite in the next few days?" Up to this point we have discussed DREAM results that use data that has already been collected and is available for the model. Real-time operations require real-time observations which are not available from all satellites and which, even if they are available, may not be able to be transferred in real time between systems at different classification levels. Geosynchronous data is the most readily available in real time, but for many satellites, data is only downloaded when the satellite is in view of the ground station.

We have configured DREAM to be run in real time with whatever data sets are available. DREAM is not dependent on any given data stream. As discussed in the previous section, data from any satellite will populate (or modify) the predicted environment in any orbit. In our example, if GPS data always lags real time by 12 hours then the DREAM output will be less accurate in the region around L=4 during that 12-hour gap but the model will still provide a global real-time specification for all orbits. DREAM does not require geosynchronous data though. If two real-time data streams are available to the model from any two satellites then DREAM will run in real-time with one or the other or both. When no real-time data is available the DREAM results for all times beyond the last observation are essentially "forecasts".

In forecast mode, DREAM uses all available data to accurately specify the current global space environment and then uses the equations in the physics model to extrapolate that environment forward in time. There is no limit to how far forward in time the model can be run but current physical models of the space environment cannot fully represent physical reality and the prediction will be less and less accurate the longer into the future it is run.

The physical model of the Earth's radiation belts that is currently used by DREAM can make predictions based on two assumptions. The first is persistence and the second is relaxation. Persistence, in any prediction, assumes that the current state will be maintained unchanged. Persistence in weather forecasting assumes that the high temperature tomorrow will be the same as the high temperature today. Generally that's a pretty good forecast but it obviously gets worse the more days in the future it is applied. Relaxation assumes that the system evolves toward a most likely state. Applied to forecasting the high temperature, say next week, relaxation might assume that the temperature will gradually transition from what was observed today to the temperature that is the historical average temperature for this time of year.

We have not yet fully tested and validated DREAM in forecast mode under either forecast assumption but preliminary results suggest that 1-week forecasts (for at least some applications) should be possible. Most radiation belt processes affect fluxes on time scales of hours to days. A 1-day persistence forecast gives a mean forecast error of a factor of 2x for a satellite at L=4 and a mean forecast error of 6x for a geosynchronous satellite (L=6.6). By five days forecasts based on persistence evolve toward values that are no better than random. The radiation belts are never static though. When there is no geomagnetic activity they don't remain constant. Rather, fluxes gradually decay. We expect, therefore, that 5- to 7-day forecasts based on relaxation should do substantially better than persistence in forecast accuracy. For more than three quarters of the time the radiation belts are in a condition of relaxation but that state is interrupted by strong enhancement events that cannot yet be accurately predicted. We note, however, that an important and valuable feature of data assimilation models such as DREAM is that it not only predicts the space environment at any point in space but it also provides a quantities uncertainty on that prediction. Therefore, DREAM forecasts, when fully validated, will not only be able to predict the space environment up to a week in the future but will also be able to quantify the confidence in that prediction as a function of time which makes DREAM much more useful for SSA applications.

7. REFERENCES

1. Blake, J.B., et al., Injection of electrons and protons with energies of tens of MeV into L<3 on 24 March 1991. *Geophys. Res. Lett. 19*: p. 821 1992.
2. Tsyganenko, N.A., A magnetospheric magnetic field model with a warped tail current sheet. *Planet. Space Sci. 37*: p. 5-20 1989.
3. Tsyganenko, N.A., H.J. Singer, and J.C. Kasper, Storm-time distortion of the inner magnetosphere: How severe can it get? *J. Geophys. Res. 108, doi:10.1029/2002JA009808*: p. 1209 2003.
4. Zaharia, S., et al., Self-consistent modeling of magnetic fields and plasmas in the inner magnetosphere: Application to a geomagnetic storm. *J. Geophys. Res. 111, A11S14, doi:10.1029/2006JA011619,* 2006.
5. Roederer, J.G., On the adiabatic motion of energetic particles in a model magnetosphere. *J. Geophys. Res. 72*: p. 981 1967.
6. Shprits, Y.Y. and R.M. Thorne, Time dependent radial diffusion modeling of relativistic electrons with realistic loss rates. *Geophys. Res. Lett. 31, L08805, doi:10.1029/2004GL019591,* 2004.
7. Chen, Y., et al., Multi-satellite Determination of the Relativistic Electron Phase Space Density at Geosynchronous Orbit: Methodology and Initial Results During Geomagnetic Quiet Times. *J. Geophys. Res. 110, A10210, doi:10.1029/2004JA010895,* 2005.
8. Chen, Y., R.H.W. Friedel, and G.D. Reeves, Multisatellite determination of the relativistic electron phase space density at geosynchronous orbit: An integrated investigation during geomagnetic storm times. *J. Geophys. Res. 112, doi:10.1029/2007JA012314,* 2007.
9. Chen, Y., G.D. Reeves, and R.H.W. Friedel, The Energization of Relativistic Electrons in the Outer Van Allen Radiation Belt. *Nature Physics. 3(9), doi:10.1038/nphys655*: p. 614-617, 2007.
10. Koller, J., R.H.W. Friedel, and G.D. Reeves, *Radiation Belt Data Assimilation and Parameter Estimation*, *Los Alamos National Laboratory Technical Report LA-UR-05-6700,:* Los Alamos, NM, 2006
11. Koller, J., et al., Identifying the radiation belt source region by data assimilation. *J. Geophys. Res. 112(A06244), doi:10.1029/2006JA012196,* 2007.
12. Koller, J., et al. Radiation Belt Data Assimilation with an Ensemble Kalman Filter. in *Proc. of 4th Space Weather Symposium,* San Antonio, TX Jan 14-18. 2007.
13. Winske, D. and S.P. Gary, Hybrid simulations of debris-ambient ion interactions in astrophysical explosions. *J. Geophys. Res. 112(A10303), doi:10.1029/2007JA012276,* 2007.
14. Belian, R.D., et al., High Z energetic particles at geosynchronous orbit during the great solar proton event of October, 1989. *J. Geophys. Res. 97*: p. 16,897 1992.
15. Cayton, T.C., et al., *Description of the BDD-IIR: Electron and proton sensors on GPS*, in *Technical Report LA-UR-98-1162*. Los Alamos National Laboratory, Los Alamos NM 87545, 1998.
16. Blake, J.B., et al., CEPPAD: Comprehensive Energetic Particle and Pitch Angle Distribution experiment on POLAR. *Space Sci. Rev. 71*: p. 531-562 1995.
17. Vette, J.I., *The AE-8 Trapped Electron Model Environment*, in *NSSDC/WDC-A-R&S 91-24*, NASA Goddard Space Flight Center, Greenbelt, Maryland, 1991.
18. Brautigam, D.H. and J.T. Bell, Crresele documentation. Interim scientific report, *Technical Report no. AD-A--301770/4/XAB, 1995-07-31*, Air Force Research Lab.,1995.